0026-895X/95/030558-10$3.00/0

MOLECULAR PHARMACOLOGY, 47:558–567, 1995.

Novel Adamantane Derivatives Act as Blockers of Open Ligand-Gated Channels and as Anticonvulsants

SERGEI M. ANTONOV, JON W. JOHNSON, NERA Y. LUKOMSKAYA, NATALYA N. POTAPYEVA, VALERIY E. GMIRO, and LEV G. MAGAZANIK

Department of Neuroscience, University of Pittsburgh, Pittsburgh, Pennsylvania 15260 (S.M.A., J.W.J.), Sechenov Institute of Evolutionary Physiology and Biochemistry, Russian Academy of Science, St. Petersburg, K-223, Russia (S.M.A., N.Y.L., N.N.P., L.G.M.), and Institute of Experimental Medicine, Russian Academy of Medical Science, St. Petersburg, A-22, Russia (V.E.G.).

Received July 19, 1994; Accepted December 7, 1994

SUMMARY

We examined the influence of the molecular structure of four novel adamantane derivatives on their ability to block the channels of nicotinic acetylcholine (ACh) and *N*-methyl-D-aspartate (NMDA) receptors. The structure of the drugs is Ad-CH_2-N^+H_2-$(CH_2)_5$-R, where Ad is adamantane and R was varied from ammonium (IEM-1754) to *tert*-butyldimethylammonium (IEM-1857) radical. The compounds induced double-exponential decays of postsynaptic currents in frog muscles and flickering of NMDA-activated channels, suggesting that each drug acts as a fast open-channel blocker at both types of receptors. The equilibrium dissociation constants (K_d) of the drugs for ACh-activated channels at −80 mV were similar, whereas the K_d values for NMDA-activated channels at −80 mV were 2–10 times lower. Several observations suggested that occupation of either type of channel by these compounds inhibited channel closure; the time constant (τ) of the slow component of the decay of postsynaptic currents in the presence of each compound was greater than the control τ, the IC_{50} of IEM-1754 for inhibition of NMDA-activated whole-cell currents was >20 times larger than its K_d for the open channel, and a transient increase in NMDA-activated whole-cell currents was observed after washout of IEM-1754. Thus, these drugs appear to act on nicotinic ACh and NMDA receptors via similar mechanisms, although the voltage dependence of block suggested that the drugs bind at a more superficial site in the ACh-activated channel. All compounds also potently prevented NMDA-induced convulsions in mice. The ED_{50} of IEM-1754 was 4 times lower than the ED_{50} of MK-801.

Channel-blocking drugs comprise an important class of pharmacologically active compounds. Their modes of action have been extensively studied, both to provide insight into the mechanisms of channel blockade and to provide information about the functional organization and structure of ligand-gated channels. Drugs that block the channel of the NMDA receptor also have the potential to be of therapeutic utility. Hyperfunction of these receptors is associated with epileptic states (1) and with some forms of neurotoxicity that result from acute insults or chronic degenerative states (2). Administration of uncompetitive antagonists may provide a pharmacological approach for reducing the deleterious effects of such pathological states.

The therapeutic utility of drugs that block the NMDA-activated channel will undoubtedly depend on the characteristics of their block. It is known that the commonly used, NMDA-activated channel blockers MK-801, phencyclidine, and ketamine, although useful pharmacological tools, induce cell swelling and eventual cell death in the cortex (2). In addition, phencyclidine and ketamine induce a behavioral state in humans that strongly resembles schizophrenia (3, 4). It has been hypothesized (5–7) that these adverse effects may be related to the slow rate of dissociation of these drugs from the NMDA-activated channels (8) or to the ability of each of these drugs to be trapped in the channel (8).

Memantine (1-amino-3,5-dimethyladamantane), an adamantane derivative that blocks NMDA-activated channels, is clinically well tolerated (9). It differs from MK-801, phencyclidine, and ketamine in several respects; it has an unrelated chemical structure, its dissociation kinetics are faster (6), and it may have a lesser tendency to be trapped in the channel (10). It is not known which, if any, of these differences may explain its reduced adverse effects. It seems reasonable, however, to search for and characterize new adamantane derivatives that act as blockers of the NMDA-

This work was supported by National Institutes of Health Grants MH45817, MH00944, and MH45156 to J.W.J. and by Russian Fundamental Science Foundation Grant 93-04-7466 to L.G.M.

ABBREVIATIONS: NMDA, *N*-methyl-D-aspartate; ACh, acetylcholine; KA, kainic acid; AMPA, α-amino-3-hydroxy-5-methyl-4-isoxazolepropionic acid; MK-801, (+)-5-methyl-10,11-dihydro-5*H*-dibenzo[*a*,*d*]cyclohepten-5,10-imine; EPC, endplate current; V_m, membrane voltage; HEPES, 4-(2-hydroxyethyl)-1-piperazineethanesulfonic acid; EGTA, ethylene glycol bis(β-aminoethyl ether)-*N*,*N*,*N*′,*N*′-tetraacetic acid; nACh, nicotinic acetylcholine.

activated channel, because they may lead to the creation of potent and more safely administered drugs.

We describe here the channel-blocking activity of a series of structurally related derivatives of adamantane. It has been shown previously that 1-trimethylammonio-5-(1-adamantanemethylammonio)pentane blocks open glutamate-activated postsynaptic channels in the neuromuscular junctions of blowfly larvae (11). We have used this compound and a related series of newly synthesized compounds to study how the structure of the distal cationic group (bound to the 1-position of the pentane radical) of these compounds affects blocking activity. Our first series of experiments revealed that the IEM drugs act as open-channel blockers of nACh receptors of frog muscles. We then compared the action of these drugs on NMDA receptors with their action on nACh receptors. Our data indicate that they block the NMDA-activated channel via a similar mechanism but with higher affinity and that the highest affinity drug (IEM-1754) is a relatively ineffective antagonist of non-NMDA glutamate responses. Because the characteristics of the IEM drugs suggested that they could be of clinical utility, we performed a third series of experiments that demonstrated that the drugs act as potent anticonvulsants *in vivo*. Some of the data concerning the fast blockade of NMDA-activated channels have been presented previously in preliminary form (12).

Materials and Methods

EPC Recording from Frog Neuromuscular Junction

Preparation and solutions. The isolated neuromuscular preparation of the sartorius muscle of the frog (*Rana temporaria*) was studied at room temperature (20–25°). The preparation was pinned in the chamber and perfused continuously with Ringer solution (115 mM NaCl, 2 mM KCl, 0.9 mM $CaCl_2$, 6 mM $MgCl_2$, 2.4 mM $NaHCO_3$; pH adjusted to 7.2–7.4 with HCl). In this solution electrical stimulation of the motor nerve did not evoke muscle contractions. Before recordings were begun, the preparations were allowed to equilibrate for 30 min. Preparations were superfused at approximately 1 ml/min with the indicated concentration of drugs dissolved in the Ringer solution.

Data recording and analysis. EPCs were evoked by motor nerve stimulation at a frequency of 0.2 Hz. EPCs of frog muscle fibers were recorded with conventional two-electrode voltage-clamp methods. Glass electrodes (resistance, 3–5 MΩ) were filled with 2.5 M KCl. The residual voltage change during an EPC was <0.2% of the peak amplitude of postsynaptic potentials recorded in the current-clamp configuration. The recorded currents were low-pass filtered at 3 kHz and digitally sampled at 25 kHz.

Ten to 20 individual postsynaptic current responses were sampled, averaged, analyzed on-line with locally written analysis programs, and stored for further off-line analysis. Amplitudes and decay time constants of EPCs at V_m values from −50 to −140 mV were measured. Two different algorithms were used to fit the double-exponential decay of EPCs. For most fits, first a slow exponential component was fit by eye to the late portion of the EPC. The fast exponential component was then fit by eye after subtraction of the slow exponential component from the EPC decay data. The accuracy of this procedure was verified in about one third of the experiments by double-exponential fitting performed using an iterative curve-fitting procedure described by Dempster (13). Best fit was determined by the parameter values that minimized the summed squared error between data and the fit curve. The time constants of exponential components determined by the two methods were consistent to within 1–5%. Measurements were repeated every 5 min during a control period of 20 min and during an experimental period of 30 min after drug application.

Single-Channel and Whole-Cell Recording from Rat Brain Neurons

Preparation and solutions. Experiments was performed at room temperature on primary cultures of neurons from embryonic rat brain cortex. Cultures were prepared using a modification of the method described by Dichter (14). Pregnant Sprague-Dawley rats were sacrificed by CO_2 inhalation at 16 days after conception, and brain cortices were obtained from 10–12 embryos. Cortices were incubated in growth medium (83% minimal essential medium, 24 mM D-glucose, 18 mM HEPES, 1.9 mM L-glutamine) with 0.03% trypsin for 40 min at 37° and then in Ca^{2+}- and Mg^{2+}-free Earle's balanced salt solution for 40 min at 37°. Cells were dissociated by trituration with a fire-polished Pasteur pipette, and debris was removed by filtration through lens paper. Cell viability was estimated using trypan blue exclusion, and a plating suspension of 200,000–250,000 cells/ml was prepared in 80% growth medium/10% calf serum/10% fetal bovine serum. Three milliliters of the plating suspension were plated onto 35-mm plastic dishes, each of which contained three 15-mm-diameter coverglasses that had been coated with rat tail collagen and poly-L-lysine. Five days after dissociation, cultures were treated with mitotic inhibitors (20 μg/ml 5′-fluoro-2′-deoxyuridine plus 50 μg/ml uridine) for 36–48 hr, to reduce proliferation of non-neuronal cells. After treatment with mitotic inhibitors, cells were fed three times each week with 90% growth medium/10% calf serum. Cells were used for patch-clamp experiments after 15–35 days in culture.

The bathing solution used for outside-out single-channel and whole-cell recordings consisted of 140 mM NaCl, 2.8 mM KCl, 1.0 mM $CaCl_2$, 10 mM HEPES, and 0.0002 mM tetrodotoxin; the pH was adjusted to 7.2 with NaOH. The intrapipette solution consisted of 120 mM CsF, 10 mM CsCl, 10 mM EGTA, and 10 mM HEPES; the pH was adjusted to 7.2 with CsOH.

Data recording and analysis. Patch-clamp recordings were carried out on the stage of an inverted microscope with phase-contrast optics. Gigaohm seals were obtained with Sylgard-coated glass pipettes (resistance, 4–5 MΩ) for outside-out patch recordings and with glass pipettes (resistance, 2–3 MΩ) for whole-cell voltage-clamp recordings (15). After outside-out patch formation, the tip of the patch electrode was placed in front of the mouth of a perfusion tube. Patches were perfused with the indicated concentrations of drugs dissolved in the bathing solution. Whole-cell currents were activated by application of the indicated solutions with a multibarrel fast perfusion system similar to that described (16).

Single-channel and whole-cell currents were recorded using an Axopatch 200 or an Axopatch-1D patch-clamp amplifier (Axon Instruments, Foster City, CA). Currents were filtered at 10 kHz (−3-dB, four-pole, low-pass Bessel filter), digitized at 44 kHz, and recorded on video tape using a Neuro-Corder DR-890 pulse code modulator adapter (Neuro Data Instruments, New York, NY) and a videocassette recorder. For analysis, the single-channel currents were filtered at 4 kHz (−3-dB, eight-pole, low-pass Bessel filter) and digitally sampled at 10 kHz, and the whole-cell currents were filtered at 100 Hz and digitally sampled at 200 Hz. Sampling was performed with a Labmaster data acquisition system and pClamp software (Axon Instruments).

Single-channel data were collected in 30–60-sec blocks and then were edited and analyzed with the Channel Analysis program (RC Electronics, Goleta, CA). To plot distributions of dwell times, openings and closings of channels were detected using a 50% threshold criterion (17). Histograms of the duration of open and closed events were constructed with square root versus log time plots (18) and fitted with the maximum log likelihood method. Time constants were corrected assuming that events shorter than the dead time of the filter (0.179/filter frequency) were missed (17). Each drug was inves-

tigated over a 10-fold concentration range. Higher drug concentrations were not used because at higher concentrations a substantial fraction of open durations became too brief to be fully resolved under the recording conditions used.

In whole-cell recordings, the control steady state current amplitude ($I_{Control}$) was measured during the plateau phase of the response to a 10–20-sec application of agonist. The response amplitude (I_B) was measured at the end of a 10-sec application of agonist plus the indicated concentration of the test compound. The response amplitude during application of the test compound was normalized to the amplitude of the control agonist response. Concentration-inhibition curves were fitted with the equation $I_B = I_{Control}/[1 + ([B]/IC_{50})^{n_H}]$, where [B] is the blocker concentration, IC_{50} is the blocker concentration at which I_B equals 50% of $I_{Control}$, and n_H is a parameter reflecting the steepness of the curve, which has the same meaning as the Hill coefficient.

All quantitative data are expressed as mean ± standard deviation. Data for $n = 2$ were not subjected to statistical analysis. When t tests were used, they were always two-tailed.

Convulsions Induced in Mice by NMDA and Other Convulsants

Adult albino male mice (bred from Swiss mice) weighing 18–22 g were used to measure anticonvulsant activity of channel blockers. All animals were fed a standard diet. All applications of both convulsants and anticonvulsants were as intracerebroventricular injections into the lateral ventricle, using a semiautomatic apparatus, as described by Vanecek *et al.* (19). The injected drugs were dissolved in saline (0.9% NaCl), and the pH was adjusted to 7.4–7.6 with NaOH. Convulsant, i.e., NMDA (0.06 μg/mouse), KA (0.2 μg/mouse), quinolinic acid (5.0 μg/mouse), nicotine (4.0 μg/mouse), or pentylenetetrazole (200 μg/mouse), was injected, in a volume of 5 μl, 5 min after the injection of the anticonvulsant drug under study. Ten mice from a large group of 100–120 mice that were raised together were tested with one of the convulsants at the concentration indicated above. The large group was used for subsequent tests of anticonvulsant activity only if a convulsive response was evoked in eight or nine of the 10 mice. This procedure (test of the convulsant on a sample of 10 mice from the large group of mice) was repeated between anticonvulsant experiments to ensure consistent responses. Each mouse was subjected to only a single injection of convulsant. In control mice, 5 μl of saline were injected instead of the convulsant drugs; this procedure never produced convulsions. The ability of the anticonvulsants to prevent the agonist-induced convulsions was examined by establishing ED_{50} values and 95% confidence limits by means of the method of Litchfield and Wilcoxon (20). Four or five doses of the anticonvulsants were tested (not fewer than 20 animals/dose) to plot the dose-response curve for calculation of ED_{50}.

Drugs

IEM drugs were synthesized at the Institute of Experimental Medicine RAMS (St. Petersburg, Russia). Purity of the IEM drugs was tested by elementary analysis and chromatography. AMPA and MK-801 were obtained from Research Biochemicals (Natick, MA) and nicotine from Aldrich (Milwaukee, WI). Other drugs were from Sigma Chemical Co. (St. Louis, MO). All drugs were kept frozen in stock solutions at concentrations of 0.2–100 mM and were diluted to the indicated concentrations before use.

Results

Structures of the IEM drugs. The four drugs studied differ in the structures of the distal cationic radical bound in the 1-position to 5-(1-adamantanemethylammonio)pentane. These radicals were ammonium for IEM-1754, trimethylammonium for IEM-1460, isopropyldimethylammonium for IEM-1592, and *tert*-butyldimethylammonium for IEM-1857 (Table 1).

Block of Cholinergic Postsynaptic Currents

We began our investigation of the channel-blocking activity of the IEM drugs by measuring their effects on the kinetics of EPCs at the frog neuromuscular junction. This preparation has been extensively used to investigate the mechanism of channel block of a variety of drugs (see Ref. 21). The decay (90–10% of peak amplitude) of EPCs evoked in frog muscle fibers by motor nerve stimulation was well fitted by a single-exponential function (time constant of τ_c) under control conditions (Fig. 1). τ_c was voltage dependent, increasing with hyperpolarization. Application of any of the IEM compounds at concentrations of 10–100 μM induced a concentration-dependent depression of the peak EPC amplitude (Fig. 2A) and a concentration-dependent change in the decay, which in the presence of drug became better fitted by a double-exponential function (Figs. 1B and 2B). Double-exponential fits to the decay of EPCs in the presence of each compound yielded time constants for the fast (τ_f) and slow (τ_s) components of the decay of the EPC (Fig. 2B). Extrapolation of each exponential component of the fit to the time of peak current yielded the values for the amplitude of each component (A_f and A_s).

We observed that τ_f was consistently faster than τ_c, whereas τ_s was consistently slower than τ_c. An increase in the concentration of each compound resulted in a decrease of τ_f and an increase of τ_s (Fig. 2B). These data strongly support the idea that the IEM compounds act as open-channel blockers that follow the sequential scheme (22–25)

$$A_nR \rightleftharpoons A_nR^* + B \underset{k_-}{\overset{k_+}{\rightleftharpoons}} A_nR^*B \quad (1)$$

where A_nR is the receptor with all agonists bound and the channel closed, A_nR^* is the receptor with all agonists bound

TABLE 1
Structures of channel blockers studied

Compound	Molecular structure[a]	Chemical name
IEM-1754	$[H_3N^+\text{-}(CH_2)_5\text{-}N^+H_2CH_2Ad]\cdot 2Br^-$	1-Ammonio-5-(1-adamantanemethylammonio)pentane dibromide
IEM-1460	$[(CH_3)_3N^+\text{-}(CH_2)_5\text{-}N^+H_2CH_2Ad]\cdot 2Br^-$	1-Trimethylammonio-5-(1-adamantanemethylammonio)pentane dibromide
IEM-1592	$[(CH_3)_2CH(CH_3)_2N^+\text{-}(CH_2)_5\text{-}N^+H_2CH_2Ad]\cdot 2Br^-$	1-Isopropyldimethylammonio-5-(1-adamantanemethylammonio)pentane dibromide
IEM-1857	$[t\text{-}(CH_3)_3C(CH_3)_2N^+\text{-}(CH_2)_5\text{-}N^+H_2CH_2Ad]\cdot 2Br^-$	1-*tert*-butyldimethylammonio-5-(1-adamantanemethylammonio)pentane dibromide

[a] Ad, adamantane ().

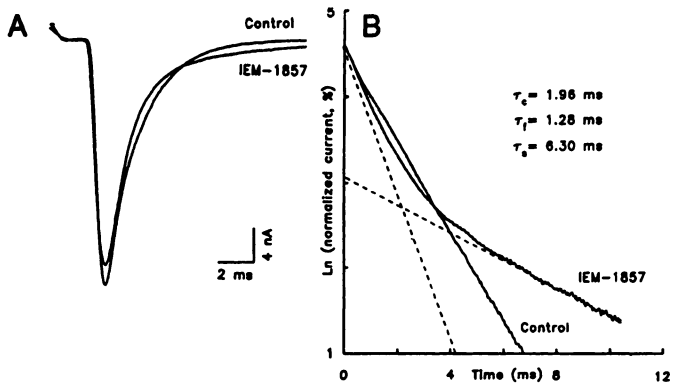

Fig. 1. Effect of 10 μM IEM-1857 on the EPCs of the frog neuromuscular junction. A, EPCs recorded at −130 mV under control conditions (EPC of larger peak amplitude) and after application of the drug (EPC with smaller amplitude, slower return to base-line). B, Semilogarithmic plot of the normalized decays (time 0 defined as time of 90% of peak amplitude) of the EPCs shown in A. *Solid lines*, data recorded under control conditions and in the presence of IEM-1857. *Dashed lines*, slow and fast exponential components determined by a double-exponential fit to the EPC decay in the presence of IEM-1857.

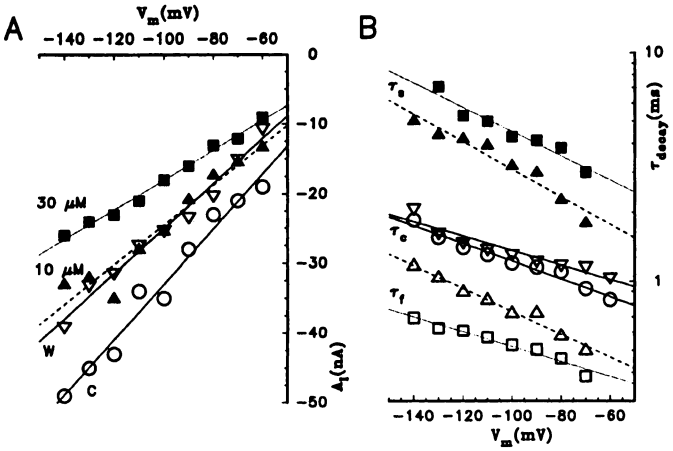

Fig. 2. Dependence on V_m and drug concentration of the effect of IEM-1857 on the EPCs recorded in the frog neuromuscular junction. A, Effect on EPC amplitude (A_f). ○, Under control conditions (*C*); ▲, in the presence of 10 μM IEM-1857; ■, in the presence of 30 μM IEM-1857; ▽, after 20-min washout of the drug (*W*). B, Effect on EPC decay time constant. ○, Under control conditions (τ_c); ▲ and △, in the presence of 10 μM IEM-1857; ■ and □, in the presence of 30 μM IEM-1857; ▲ and ■, slow component of decay (τ_s); △ and □, fast component of decay (τ_f); ▽, after 20-min washout of the drug. *Lines*, linear regressions through the points. All data are from a single experiment.

and the channel open, B is the channel-blocking molecule, A_nR^*B is the activated receptor with channel blocked, k_+ is the rate constant of association (blocking reaction), and k_- is the rate constant of dissociation (unblocking reaction). In the presence of blockers that follow eq. 1, τ_f is faster than τ_c because the channel open duration is shortened by the entry of blocker into the open channel. However, progressive prolongation of the single-channel burst duration (the time spent oscillating between states A_nR^* and A_nR^*B) should occur as blocker concentration increases. The slow exponential component induced in the double-exponential decay of EPCs reflects the prolongation by blocker of single-channel burst duration (25).

In accord with eq.1, the rate constants of block for each of the compounds (k_+ and k_-) can be calculated using τ_c, τ_f, τ_s, and the ratio of the amplitudes of the exponentials obtained from the double-exponential fits to the decay of EPCs (23). The k_- was estimated from the equation $k_- = [1/\tau_s + A_s/(A_f \cdot \tau_f)]/(1 + A_s/A_f)$. The k_+ was estimated from the equation $k_+ = (1/\tau_s + 1/\tau_f - 1/\tau_c - k_-)/[B]$. The channel-blocking rates and equilibrium constants for each IEM compound obtained at two levels of V_m are presented in Table 2. The values of k_+ for IEM-1754, -1592, and -1857 did not differ significantly from each other; for IEM-1460, however, k_+ was approximately 2-fold higher. The values of k_- were also similar for IEM-1754, -1592, and -1857 but were significantly higher for IEM-1460, resulting in a K_d that was slightly but significantly lower than the K_d values for the other IEM drugs. Thus, the results suggest that the compounds studied are open-channel blockers of nACh receptors with moderate potency (K_d in the range of 10–50 μM) and relatively fast rates of dissociation (450–700 sec^{-1}). When the ACh-activated channel is blocked by any IEM drug its closure is inhibited, although with the present data we cannot determine whether channel closure is fully prevented. Block induced by the drugs was weakly voltage dependent (Table 2); the K_d values for all four drugs decreased with hyperpolarization, and the decreases of the K_d values of both IEM-1754 and IEM-1857 were significant.

Blockade of NMDA-Activated Currents

Memantine, a derivative of adamantane, has been shown to block open NMDA-activated channels (6). The adamantane derivative amantadine acts as an open-channel blocker of both nACh receptors of frog muscle (24) and of NMDA receptors (10). We investigated the possibility that the IEM compounds also can inhibit, by similar mechanisms, both NMDA and nACh receptors. To permit quantitative determination of the rate constants of block, we began by studying NMDA response inhibition using single-channel recording techniques.

"Flickering block" of NMDA-activated channels. The application of 10 μM NMDA plus 10 μM glycine (control conditions) to outside-out patches induced single-channel currents. We attribute these currents to the activity of NMDA-activated channels, based on single-channel conductance and kinetics and the absence of openings in the absence of NMDA at all of the V_m values studied. All four IEM drugs affected the kinetic properties of single-channel currents. Fig. 3 illustrates single-channel currents under control conditions and in the presence of each of the compounds. Under control conditions, relatively long-duration openings interrupted by infrequent brief closures were observed. In the presence of each of the IEM compounds, channel openings were interrupted frequently by brief closures that were not observed without the compounds. This flickering block (21) strongly suggests that these substances act as fast blockers of the NMDA-activated channel. The block resembles the block by extracellular Mg^{2+} observed at similar V_m values (26–28). It is unlikely, however, that there was significant Mg^{2+} contamination of our solutions, because the mean open times of NMDA-activated channels under control conditions at +40 mV (5.04 ± 0.83 msec, n = 7) and at −80 mV (4.05 ± 0.68 msec, n = 8) were not significantly different. In addition, we measured by flame spectrophotometry the Mg^{2+} concentration in the bathing solutions with 10 μM NMDA, 10 μM glycine, 0.2 μM tetrodotoxin, and 30 μM IEM-1460, -1592, or

TABLE 2

Rate and equilibrium constants of open-channel block of NMDA and nACh receptors at two membrane voltages

Mean ± standard deviation values (n = 3–7) or mean values (n = 2) are presented. The k_+ for NMDA-gated channels was calculated for each patch as the slope of the dependence of $1/\tau_0$ on [B]. Values of k_+ for ACh-gated channels measured at different blocker concentrations were pooled to calculate mean values of k_+ in each experiment. For both receptors, values of k_- measured at different blocker concentrations were pooled to calculate mean values of k_-.

Drug	V_m	$k_+(\cdot 10^7)$		k_-		K_d	
		NMDA	ACh	NMDA	ACh	NMDA	ACh
	mV	M^{-1} sec^{-1}		sec^{-1}		μM	
IEM-1754	−80	22.3 ± 3.0[a]	2.4 ± 0.5	775 ± 214	532 ± 57	2.8 ± 0.6[a]	25 ± 5
	−120	36.1 ± 0.8[a,b]	2.9 ± 0.5	123 ± 15[b]	475 ± 86	0.4 ± 0.1[a,b]	17 ± 3[d]
IEM-1460	−80	4.6	5.4 ± 1.3[f]	776	696 ± 79[g]	15.8	13 ± 3[g]
	−120	9.5	7.2	171	858	1.72	12
IEM-1592	−80	4.6	1.9 ± 0.5	820	453 ± 27	16.7	27 ± 5
	−120	11.2	2.2 ± 0.4	274	460 ± 43	2.44	21 ± 2
IEM-1857	−80	4.9 ± 0.6	1.7 ± 0.3	662 ± 110	543 ± 38	13.5 ± 4.5	49 ± 20
	−120	12.4 ± 2.2[b]	2.0 ± 0.3	370 ± 98[c]	354 ± 47[e]	3.0 ± 0.9[b]	18 ± 3[d]

[a] Value for IEM-1754 differs from the corresponding value of IEM-1857 at the same V_m (t test for independent groups, $p < 0.01$).
[b,c] Value differs from the value obtained for the same compound at V_m = −80 mV (t test for correlated groups; b, $p < 0.01$; c, $p < 0.05$).
[d,e] Value differs from the value obtained for the same compound at V_m = −80 mV (t test for correlated groups; d, $p < 0.05$; e, $p < 0.01$).
[f,g] Value differs from the corresponding value at the same V_m for other compounds (one-way analysis of variance; f, $p < 0.01$; g, $p < 0.05$).

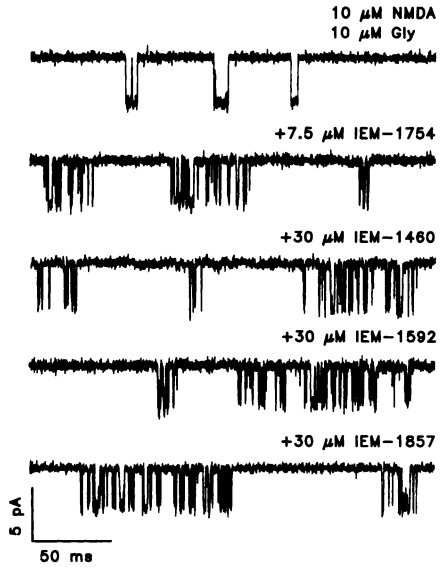

Fig. 3. Flickering block of NMDA-activated single-channel currents induced by the compounds studied. *Traces*, single-channel currents recorded with 10 μM NMDA plus 10 μM glycine (*Gly*) at −80 mV, in the absence (*upper trace*) and in the presence (*lower four traces*) of each compound (the drugs and concentrations added are indicated directly above the traces). Recordings in the absence of drug and in the presence of IEM-1460 were obtained from the same patch.

-1857. In each case, the Mg^{2+} concentration was below detectable levels (about 2 μM).

Mechanism of block. The data of Fig. 3 suggest that the IEM compounds act as blockers of the open NMDA-activated channel. If this suggestion is correct, then our single-channel data should conform to the following predictions (22, 25): (i) mean open time should be decreased by the drug, but the number of exponential components in the open-time histogram should be the same in the absence and presence of drug; (ii) k_+ should equal $(1/\tau_{O,B} - 1/\tau_{O,C})/[B]$, where $\tau_{O,C}$ is the mean open time under control conditions and $\tau_{O,B}$ is the mean open time in the presence of channel blocker at a concentration of [B]; (iii) k_- should not depend on [B] and should equal $1/\tau_B$, where τ_B is the mean duration of the blocked state; and (iv) the mean duration of long closed times (reflecting residence times in states to the left of A_nR^*) should not be affected by the channel blocker.

To determine whether the four compounds act by blocking the open NMDA-activated channel and, if so, to quantify the rate constants of block, we measured the following kinetic parameters at −80 and −120 mV: τ_O, the mean duration of channel openings under control conditions or in the presence of blocker, which can be used to estimate $\tau_{O,C}$ and $\tau_{O,B}$; $\tau_{S,C}$, the mean duration of short closures under control conditions; $\tau_{A,C}$, the mean duration of additional short closures in the presence of the compounds, which can be used to estimate τ_B; and $\tau_{L,C}$, the mean duration of long closures between bursts.

Open-time histograms were generally well fit by single-

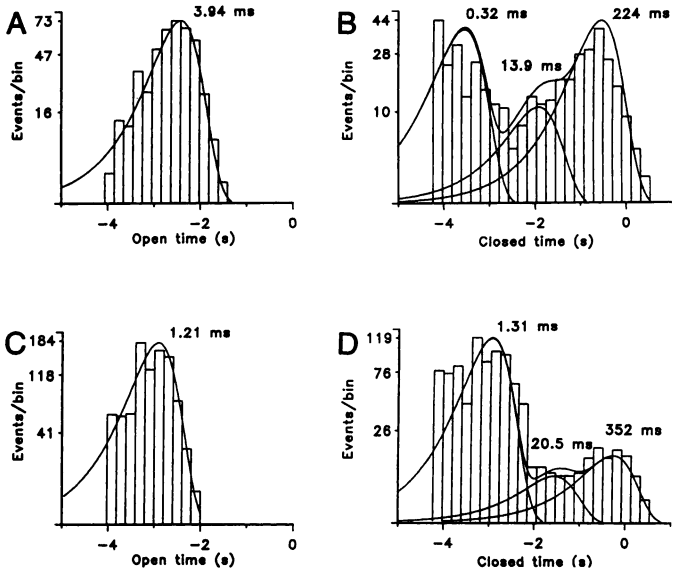

Fig. 4. Effect of IEM-1857 on kinetics of NMDA-activated single-channel currents induced in outside-out patches by application of 10 μM NMDA plus 10 μM glycine at −80 mV. A, Distribution of open times under control conditions; B, distribution of closed times under control conditions; C, distribution of open times in the presence of 10 μM IEM-1857; D, distribution of closed times in the presence of 10 μM IEM-1857. All histograms are presented as square root versus log time plots. *Lines*, single- or triple-exponential fits to the data. *Numbers shown above the exponential components*, time constants. All plotted data were obtained from the same patch.

exponential functions both under control conditions (Fig. 4A) and in the presence of each compound (Fig. 4C). In some experiments a second, very brief, open-time component, which we did not attempt to fit, was observed. Up to three exponential components have been required to fit open-time histograms when NMDA receptors are activated by glutamate (29). However, histograms in the presence of NMDA are generally adequately fit by a single-exponential function (27, 28). The value of τ_O at −80 mV in the presence of each IEM compound (e.g., Fig. 4C) was smaller than τ_O under control conditions (Fig. 4A; see above), as would be expected of an open-channel blocker (prediction i). In the presence of 30 μM IEM-1857, -1592, and -1460, the values of τ_O were 0.64 ± 0.02 msec (n = 4), 0.62 msec (n = 2), and 0.64 msec (n = 2), respectively. IEM-1754 at 7.5 μM decreased τ_O to 0.65 ± 0.10 msec (n = 6).

Closed-time histograms under control conditions exhibited a multiexponential distribution (Fig. 4B) (29). Control closed-time histograms were generally adequately fit with three exponential components. The presence of any of the compounds induced an additional component in the closed-time distribution (e.g., Fig. 4D). For confident measurement of the time constant of the additional component ($\tau_{A,C}$), it had to be distinguished from the closed-time components present under control conditions. It was often not possible to distinguish $\tau_{S,C}$ and $\tau_{A,C}$ under the experimental conditions used here; $\tau_{S,C}$ is relatively fast (0.32 msec in Fig. 4B; see also Ref. 28), and the distribution of short closures often overlapped with the distribution of the blocked state. However, when sufficiently high concentrations of the compounds were used, channel block occurred much more frequently than brief closures. Comparison of the amplitudes of the exponential fits in Fig. 4, B and D, demonstrates that the blocked state was observed far more frequently than short closures under control conditions. Because of the much higher frequency of channel-blocking events, we were able to accurately measure the value of $\tau_{A,C}$ despite the presence of short closures.

The IEM drugs induced a concentration-dependent decrease of τ_O. Fig. 5A shows qualitatively that at −80 mV the frequency of block appeared to increase with the concentration of IEM-1857. Plots of the value of $1/\tau_O$ as a function of drug concentration could be well approximated by a straight line (Fig. 5B). This is consistent with channel block prediction ii, which also states that the slope of the line should be equal to the blocking rate constant k_+. At each V_m tested, the slope of such plots for IEM-1754 was significantly greater than those for IEM-1460, -1592, and -1857. This suggests that the blocking rate for IEM-1754 is substantially higher than the corresponding rates for IEM-1460, -1592, and -1857, which were nearly identical to each other (Table 2). As Fig. 5C and Table 2 show, the rate constant of dissociation (k_-) did not depend either on the concentration of channel blocker (channel block prediction iii) or on the channel blocker molecular structure. The higher value of k_+ for IEM-1754 therefore leads to a lower equilibrium dissociation constant (K_d) value, calculated as the ratio $K_d = k_-/k_+$ (Table 2). In accord with prediction iv, none of the compounds affected $\tau_{L,C}$; the ratio of $\tau_{L,C}$ in the presence of the compounds to $\tau_{L,C}$ under control conditions was 1.34 ± 1.05 (n = 16). Under control conditions $\tau_{L,C}$ ranged between 48 and 990 msec, with a mean value of 301 msec (n = 16).

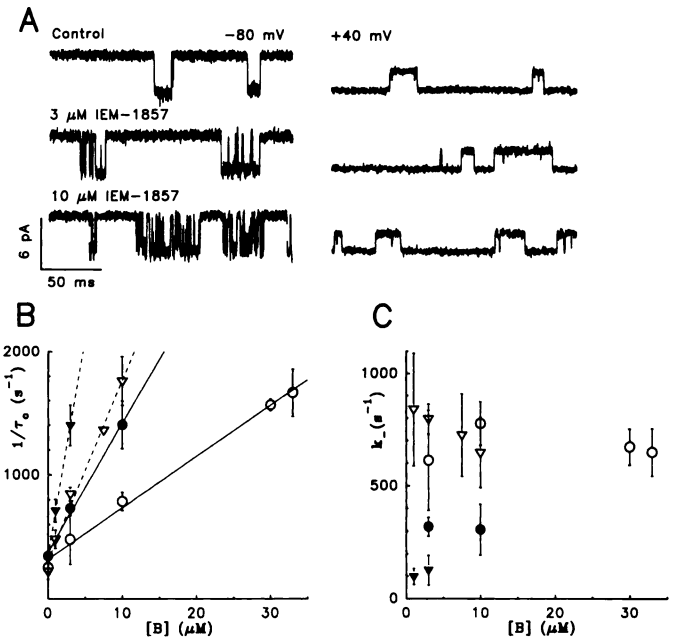

Fig. 5. Dependence of blocking kinetics on concentration of channel blockers and on membrane potential. A, Traces show single-channel currents recorded with 10 μM NMDA plus 10 μM glycine in the presence of 0 (*upper*), 3 (*middle*), or 10 (*lower*) μM IEM-1857, at −80 (*left*) or +40 mV (*right*). B, Reciprocal mean open time ($1/\tau_o$) is plotted as a function of blocker concentration ([*B*]) at −80 and −120 mV. *Lines*, linear regressions through the *points*. *Inverted triangles*, IEM-1754; *circles*, IEM-1857. *Open symbols*, V_m = −80 mV; *filled symbols*, V_m = −120 mV. *Symbols with error bars*, means ± standard deviations of three to five experiments. C, The rate constant of blocker dissociation (k_-) is plotted as a function of blocker concentration at −80 and −120 mV. The k_- was calculated from the equation $k_- = 1/\tau_B$. *Symbols* have same meanings as in B.

Voltage dependence of block. Fig. 5A shows qualitatively that block of NMDA-activated channels by the compounds is voltage dependent; flickering block induced by IEM-1857 at −80 mV was not visible when the patch was depolarized to +40 mV. To quantitate the voltage dependence of the rate constants of open-channel block and to compare the voltage dependence of these constants with that of the block of nACh receptors, kinetic measurements were made at −120 mV as well as at −80 mV. Fig. 5B shows that $1/\tau_O$ for IEM-1754 and -1857 at each tested concentration was greater at −120 mV than at −80 mV, resulting in a greater slope of concentration dependence at −120 mV and a greater calculated value of k_+. Hyperpolarization increased the blocking rates of each blocker (Table 2). This is the direction of voltage dependence that would be expected for an extracellularly applied channel blocker with a positive charge. The effect of hyperpolarization on k_- was opposite; k_- decreased with hyperpolarization (Fig. 5C; Table 2). This voltage dependence of k_- suggests that, when dissociating, the blockers preferentially return to the extracellular medium. Table 2 summarizes the parameters of channel-blocking activity at −80 mV and at −120 mV and allows quantitative comparison of the block of NMDA-activated and ACh-activated channels. It is clear that block by each compound of NMDA-activated channels is strongly voltage dependent.

Apparent dissociation constant from whole-cell experiments. Although the data presented above demonstrate that the IEM drugs block open NMDA-activated channels,

they do not allow determination of the pathway(s) through which the channel can leave the open blocked state (A_nR^*B). Equation 1 postulates that the binding of channel blocker prevents channel closure. If this postulate is correct, then the IC_{50} of the blocker measured in whole-cell experiments should be greater than the open-channel K_d of the blocker (22). The difference should be greatest when IC_{50} is measured in the presence of low agonist concentrations. If channel closure is unaffected by the binding of blocker, however, then the open-channel K_d (Table 2) and whole-cell IC_{50} may be equal. Equation 1 therefore predicts that the IC_{50} of inhibition of whole-cell currents by the IEM compounds should be greater than the K_d measured from single-channel experiments. The difference should be accentuated at relatively low NMDA concentrations.

In accord with this prediction, concentrations of IEM-1754 much higher than the K_d value measured in single-channel experiments were necessary to induce substantial inhibition of whole-cell currents in the presence of 10 μM NMDA (Fig. 6A). The value of IC_{50} (60 μM) estimated from the concentration-inhibition curve (Fig. 6B) was >20 times greater than the K_d value for IEM-1754. This observation supports the conclusion that closure of the NMDA-activated channel is partially inhibited or fully prevented during channel block by IEM-1754.

Selectivity of block. The selectivity of IEM-1754 among glutamate receptors was assessed by comparing its effects on whole-cell currents evoked by the excitatory amino acids NMDA, KA, and AMPA. IEM-1754 at 100 μM had relatively little effect on currents induced by application of 30 μM KA or 20 μM AMPA, whereas it strongly blocked the current evoked by 10 μM NMDA plus 10 μM glycine (Fig. 7). The amplitudes of responses evoked by NMDA, KA, and AMPA in the presence of 100 μM IEM-1754 were 0.15 ± 0.02 (n = 4), 0.92 ± 0.09 (n = 4), and 0.92 ± 0.08 (n = 6), respectively, relative to the amplitudes of control responses. A rapidly decaying current peak after removal of IEM-1754 was consistently observed after inhibition of NMDA-activated currents (Fig. 7A; see Discussion) but was never observed after inhibition of KA- or AMPA-activated currents.

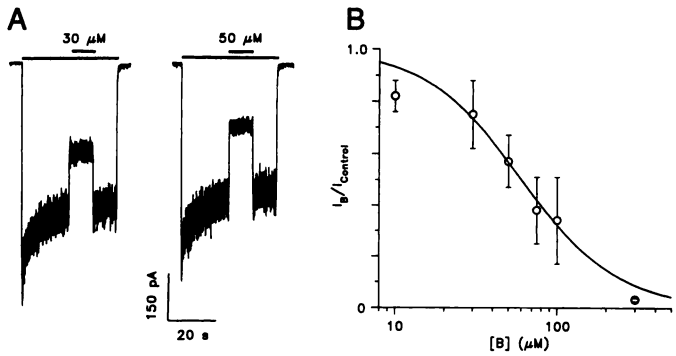

Fig. 6. Concentration-inhibition curve for block by IEM-1754 of whole-cell NMDA-activated currents at −80 mV. A, IEM-1754 at 30 and 50 μM (*bars above the traces*) decreased the amplitude of whole-cell currents evoked by the application of 10 μM NMDA plus 10 μM glycine. B, The concentration-inhibition curve of whole-cell responses evoked by the application of 10 μM NMDA plus 10 μM glycine is shown. *Symbols*, mean ± standard deviation values of three to seven cells. *Line*, best fit to the data points of the equation described in Materials and Methods. The IC_{50} of the IEM-1754 effect estimated from the fit equals 60 μM, and n_H is 1.44.

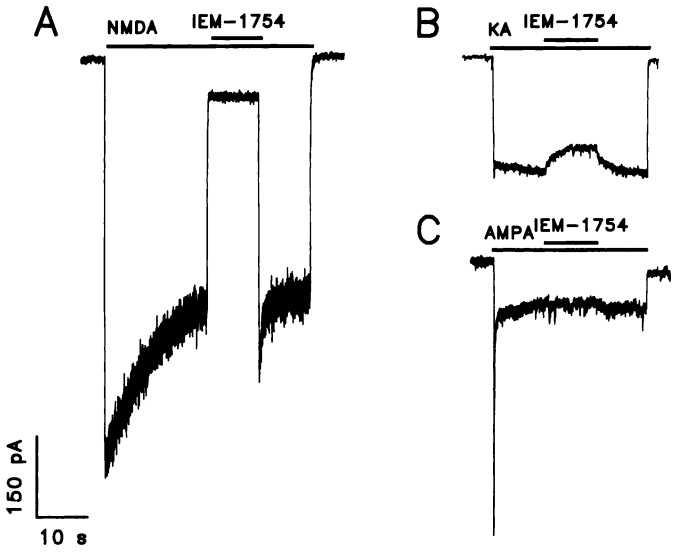

Fig. 7. Selectivity of IEM-1754 action among glutamate receptors. A, IEM-1754 at 100 μM decreased the amplitude of current evoked by the application of 10 μM NMDA plus 10 μM glycine, at −80 mV, to 13% of control value. B and C, Currents evoked by applications of 30 μM KA (B) and 20 μM AMPA (C) at −80 mV were decreased to 82% and 92% of control values, respectively. Traces shown in A and C were obtained from the same neuron. *Bars above the traces*, application protocols.

Anticonvulsant Effect

Many drugs that block the NMDA-activated channel are effective anticonvulsants in various seizure models (5). The data presented here therefore suggest that the IEM compounds may exhibit anticonvulsant activity. We investigated this possibility by measuring the ability of the IEM compounds to prevent seizures induced by a series of convulsants (Table 3). We also compared their anticonvulsant activity with that of MK-801, one of the most potent blockers of NMDA channels (8). Intracerebroventricular injection of each of the convulsants alone produced convulsions in 80–90% of mice (see Materials and Methods) within 5 min of the time of injection. Convulsions consisted of wild running or jumping and generalized clonic seizures, sometimes accompanied by tonic episodes. All adamantane derivatives studied produced clear protection against convulsions evoked by NMDA (Table 3). The ED_{50} values of IEM-1460, -1592, and -1857 did not differ significantly from that of MK-801. IEM-1754 prevented convulsions with an ED_{50} 4–9.5 times lower than that of the other IEM compounds studied and 4.5 times lower than that of MK-801. The effect of all anticonvulsants was concentration dependent up to the ED_{70}. In most experiments, increasing the dose of anticonvulsant (including MK-801) beyond the ED_{70} did not result in further protection. In contrast to the adamantane derivatives, administration of MK-801 at its ED_{50} produced obvious behavioral changes in mice (excitation, locomotion failure, and sometimes seizures) before the administration of convulsant. To study the specificity of the anticonvulsant effect, seizures were evoked by other convulsants (KA, quinolinic acid, nicotine, and pentylenetetrazole). Even at very high doses (10–50 times higher than the ED_{50} for NMDA-induced convulsions), the compounds under study were ineffective at preventing the convulsions evoked by all convulsants tested other than NMDA (Table 3).

TABLE 3

Comparison of anticonvulsant activity of IEM drugs and MK-801

Convulsants were injected into the lateral cerebral ventricle of white mice 5 min after the injection of anticonvulsant. All drugs were injected in a volume of 5 μl.

Anticonvulsant	ED_{50}				
	NMDA (0.06 μg/mouse)	KA (0.2 μg/mouse)	Quinolinic acid (5.0 μg/mouse)	Nicotine (4.0 μg/mouse)	Pentylenetetrazol (200 μg/mouse)
	nmol/mouse				
IEM-1754	0.0031[a]			>0.5	
IEM-1460	0.029			>0.5	
IEM-1592	0.025				
IEM-1857	0.013	0.5	>0.5	>0.5	>0.5
MK-801	0.014		>0.05	>0.05	

[a] Value differs significantly from other values in the same column (Litchfield and Wilcoxon method, $p < 0.05$).

Discussion

Open channel block by IEM drugs. The data presented here show that the four IEM compounds studied block open channels of nACh and NMDA receptors. Each of the drugs induced double-exponential decay of EPCs in frog muscles (Figs. 1 and 2B) and flickering of NMDA-activated single-channel currents (Fig. 3). Each of the IEM compounds decreased, in a concentration-dependent manner, the time constant of the fast component of EPC decay (Fig. 2B) and the mean open time of NMDA-activated channels (Fig. 5A). The dependence of mean open time of NMDA-activated channels on blocker concentration was linear (Fig. 5A). The rate constant of dissociation from either nACh or NMDA receptors did not depend on blocker concentration (Fig. 5B; Table 2). In addition, no changes in the mean duration of long closed times of NMDA-activated single-channel currents were observed in the presence of the IEM drug (Fig. 4, B and D). The evidence described above indicates that each of these receptors contains within its ion channel a binding site for the IEM compounds and that occupation of the binding site prevents ion flow through the channel.

Our data suggest that the sequential scheme of open-channel block (eq. 1) provides a reasonable first approximation to the dominant mechanism by which the IEM drugs interact with both nACh and NMDA receptors. The IEM drugs induced in the decay time course of EPCs a second exponential component that was slower than the decay time constant under control conditions. The time constant of the slow component became slower as the drug concentration was increased (Fig. 2B). These characteristics strongly support the idea that binding of the IEM drugs inhibits closure of ACh-activated channels. We investigated the interaction of IEM drug binding with gating of NMDA receptors by comparing the block of single-channel and whole-cell currents. As predicted by eq. 1 (22), we found that the IC_{50} of IEM-1754 obtained in whole-cell experiments (Fig. 6) was much higher than the K_d estimated from single-channel current analysis (Table 2). Fig. 7A illustrates an additional characteristic of the effect of IEM-1754 on whole-cell currents that is typical of blockers that inhibit channel closure; shortly after the rapid removal of a high concentration of IEM-1754 in whole-cell experiments, a transient current peak was consistently observed. Similar peaks have been observed in experiments with tetrabutylammonium (30), 1,2,3,4-tetrahydro-9-aminoacridine (31, 32), and 9-aminoacridine (33). The peaks generally have been attributed to the ability of these drugs to block the open channel and inhibit channel closure while blocking (31–33), although there are possible alternative explanations (30). This observation thus is consistent with the suggestion, based on comparison of whole-cell IC_{50} and single-channel K_d values, that binding of IEM-1754 inhibits channel closure. We expect that the mechanism of action of the other IEM compounds is similar, although additional data will be needed to verify this prediction. The ability of IEM-1754 (and possibly the other IEM compounds) to inhibit closure of the NMDA-activated channel contrasts with the mechanism of action of the majority of known blockers of the NMDA-activated channel (8, 10, 27, 34, 35).

Structure-activity relationships. The structure-activity relationship of these compounds revealed similarities in their actions on nACh and NMDA receptors. All of the IEM compounds exhibited similar equilibrium dissociation constants (K_d) for blockade of the open channel of the nACh receptor (Table 2). The observation that the change of the distal cationic radical from ammonium to *tert*-butyldimethylammonium did not influence blocking activity suggests that the 5-(1-adamantanemethylammonio)pentane group plays the principal role in binding to the ion channel. The ability of *n*-alkyl analogues of amantadine to block the ACh-activated channel with similar potency supports this idea (24).

Several lines of evidence suggest that the 1-adamantanemethylammonium group plays the main role in binding to the NMDA-activated channel: (i) the blocking characteristics of IEM-1460, -1592, and -1857, which have considerably different trialkylammonium radicals, are very similar (Table 2); (ii) the singly charged, NMDA-activated channel blocker memantine (1-amino-3,5-dimethyladamantane), the chemical structure of which resembles the 1-adamantanemethylammonium group of our compounds, exhibits block of the NMDA-activated channel with affinity of the same order of magnitude as that of the IEM drugs (macroscopic K_d = 6.1 μM at V_m = 0) (6); and, (iii) tetraethylammonium, the chemical structure of which resembles the distal trialkylammonium radical of our compounds, inhibits current flow through the NMDA-activated channel only at much higher concentrations (apparent K_d = 45 mM at V_m = 0) (36). IEM-1754, however, the drug with the smallest distal cationic group ($-NH_3^+$), exhibited a k_+ at least 4 times greater than that of the other drugs, whereas its k_- was not significantly different. The distal cationic group must therefore play some role in drug binding. At the V_m values tested, the association rate of IEM-1754 was unusually fast; it was comparable to that of Zn^{2+} (34) and arcaine (35) and substantially faster than that

of Mg^{2+} (27, 28), whereas the dissociation rate of IEM-1754 was slower than that of these agents. Thus, IEM-1754 has the highest affinity among these fast blockers of NMDA-activated channels.

Voltage dependence. Block of the NMDA-activated channel exhibited stronger voltage dependence than did block of the ACh-activated channel. The location of the site at which channel blockers bind can be estimated from the voltage dependence of block using the Woodhull model (37). Although the Woodhull model requires numerous assumptions that may not be satisfied during block of the NMDA-activated channel (38), estimation of electrical distance provides a useful method for comparing relative binding site locations for different substances. The mean voltage dependence of the K_d values for the IEM compounds was an e-fold change for 17 ± 5 mV (n = 4) (Table 2). Assuming that each compound binds at the same site in the NMDA-activated channel, this corresponds to $z\delta = 1.49$, where z is the charge of the molecule and δ is the fraction of the total electrical field traversed by the molecule in the process of binding. Because the IEM drugs studied can be doubly charged at physiological pH (Table 1), the appropriate value of z appears to be 2, indicating that $\delta = 0.75$. This location is similar to that estimated for memantine (6).

Interpretation of the value of δ depends on the binding conformation of the IEM compounds. Molecules with amino groups separated by more than nine carbon atoms may be able to bind in the NMDA-activated channel in a folded conformation (39). The shorter carbon chain of the IEM compounds, as well as calculations using molecular mechanics optimization algorithms,[1] suggests that these compounds block in an extended or nearly extended conformation. Our data therefore suggest that the calculated values of δ correspond to a point between the charged nitrogens when blocker is bound.

In contrast to the voltage dependence of block of the NMDA-activated channel, the K_d of block by the IEM compounds of ACh-activated channels was only weakly voltage dependent. Based on the data in Table 2, the average voltage dependence of K_d was e-fold for 75 ± 26 mV (n = 4), yielding $z\delta = 0.33$, or, with a z of 2, $\delta = 0.17$. The binding site for the IEM compounds appears to be close to the outer vestibule of the ACh-activated channel.

Anticonvulsant activity. Many drugs that block the NMDA-activated channel are effective as anticonvulsants against seizures induced by a variety of chemoconvulsants, including NMDA, picrotoxin, and bicuculline. Blockers of the NMDA-activated channel usually are weaker against convulsions induced by pentylenetetrazole (5). The selectivity of action of the IEM compounds (Table 3) suggests that block of the NMDA-activated channel is critical to the anticonvulsant activity of the IEM drugs.

Although both the open-channel K_d (Table 2) and the whole-cell IC_{50} (Fig. 6) of IEM-1754 are much higher than the estimated dissociation constant of MK-801, the anticonvulsant potency of IEM-1754 exceeded that of MK-801. The potencies of the other IEM compounds were similar to that of MK-801. One possible explanation for these observations is that the pharmacokinetics of MK-801 may be drastically different from those of the IEM compounds. This seems unlikely, for several reasons. First, the molecules are of similar size. Second, our use of intracerebroventricular injections should minimize pharmacokinetic differences, because access to the site(s) of action from the site of injection should be excellent. Finally, the short delay (5 min) between the injection of anticonvulsant and that of convulsant should have minimized differences due to potential loss of anticonvulsant from the brain.

An alternative explanation for the remarkable anticonvulsant activity of the IEM drugs is that prevention of convulsions by blockers of NMDA-activated channels may depend on the blocking rate (k_+) as well as the steady state IC_{50} (5). Effective anticonvulsant activity may require that a blocker enter the NMDA-activated channel rapidly, especially if the blocker is applied shortly before the convulsant, as in the protocol used here. The blocking rates (k_+) of the drugs under study correlate well with anticonvulsant activity. The k_+ values of IEM-1460, -1592, and -1857 at −80 mV (Table 2) are a little greater than the k_+ of MK-801 at −60 mV (2.4×10^7 M^{-1} sec^{-1}) (40), whereas the k_+ of IEM-1754 is nearly 10 times greater. The similarity between the relative blocking rates and the anticonvulsant potency of these drugs supports the idea that the rate at which a drug blocks the NMDA-activated channel may be an important determinant of its effectiveness as an anticonvulsant.

The IEM drugs possess two other traits that may prove important to their potential therapeutic utility. First, their unblocking rate (as well as their blocking rate) is fast, relative to that of most other blockers of NMDA-activated channels. Slow unblocking rates have been associated with toxicity, and it has been suggested that uncompetitive antagonists with rapid unblocking rates may be safer drugs for clinical use (5–7). Second, IEM-1754 (and possibly the other IEM drugs) inhibits channel closure and therefore cannot be easily trapped in the NMDA-activated channel. The ability of channel blockers to be trapped in the NMDA-activated channel may decrease the potential clinical utility of the drugs (6, 7). Memantine, another adamantane derivative that blocks NMDA-activated channels (6), does not prevent closure of the NMDA-activated channels (10). The most obvious structural difference between memantine and the IEM drugs is the addition to the IEM drugs of a relatively long pentane radical with a charged ammonium or trialkylammonium group. Based on this comparison, we can speculate that this side chain plays an important role in the prevention by the IEM drugs of channel closure.

These data lead us to expect that IEM-1754, or future drugs based on its structure, may be useful both as research tools and in the prevention of pathological states that result from excessive activation of glutamate receptors. The future development of more effective drugs may be aided by the information provided here on the relation between the chemical structures and the molecular pharmacology of these compounds.

Acknowledgments

We would like to thank Keith Newell for excellent technical assistance, Thomas Blanpied for useful suggestions on the manuscript, and Dr. Franklin Fuchs for help in measuring the concentration of Mg^{2+} in our solutions.

[1] D. Tichonov and L. Magazanik, unpublished observations.

References

1. Meldrum, B. S. Excitatory amino acids in epilepsy and potential novel therapies. *Epilepsy Res.* **12**:189–196 (1992).
2. Zorumski, C. F., and J. W. Olney. Excitotoxic neuronal damage and neuropsychiatric disorders. *Pharmacol. Ther.* **59**:145–162 (1993).
3. Javitt, D. C., and S. R. Zukin. Recent advances in the phencyclidine model of schizophrenia. *Am. J. Psychiatry* **148**:1301–1308 (1991).
4. Krystal, J. H., L. P. Karper, J. P. Seibyl, G. K. Freeman, R. Delaney, J. D. Bremner, G. R. Heninger, M. B. Bowers, Jr., and D. S. Charney. Subanesthetic effects of the noncompetitive NMDA antagonist, ketamine, in humans: psychotomimetic, perceptual, cognitive, and neuroendocrine responses. *Arch. Gen. Psychiatry* **51**:199–214 (1994).
5. Rogawski, M. A., and R. J. Porter. Antiepileptic drugs: pharmacological mechanisms and clinical efficacy with consideration of promising developmental stage compounds. *Pharmacol. Rev.* **42**:223–286 (1990).
6. Chen, H.-S. V., J. W. Pellegrini, S. K. Aggarwal, S. Z. Lei, S. Warach, F. E. Jensen, and S. A. Lipton. Open-channel block of *N*-methyl-D-aspartate (NMDA) responses by memantine: therapeutic advantage against NMDA receptor-mediated neurotoxicity. *J. Neurosci.* **12**:4427–4436 (1992).
7. Lipton, S. A. Prospects for clinically tolerated NMDA antagonists: open-channel blockers and alternative redox states of nitric oxide. *Trends Neurosci.* **16**:527–532 (1993).
8. MacDonald, J. F., M. C. Bartlett, I. Mody, P. Pahapill, J. N. Reynolds, M. W. Salter, J. H. Schneiderman, and P. S. Pennefather. Actions of ketamine, phencyclidine and MK-801 on NMDA receptor currents in cultured mouse hippocampal neurons. *J. Physiol. (Lond.)* **432**:483–508 (1991).
9. Ditzler, K. Efficacy and tolerability of memantine in patients with dementia syndrome. *Drug Res.* **41**:773–780 (1991).
10. Blanpied, T. A., and J. W. Johnson. Trapping open channel block and noncompetitive antagonism of NMDA responses by amantadine and memantine. *Soc. Neurosci. Abstr.* **20**:212 (1994).
11. Magazanik, L. G., S. M. Antonov, and E. V. Gmiro. Kinetics and pharmacological blockade of glutamate-activated postsynaptic ion channels. *Biol. Membr.* **1**:130–140 (1984).
12. Antonov, S. M., V. E. Gmiro, and J. W. Johnson. Adamantane derivatives induce flickering of *N*-methyl-D-aspartate (NMDA)-activated channels. *Soc. Neurosci. Abstr.* **19**:467 (1993).
13. Dempster, J. *Computer Analysis of Electrophysiological Signals.* Academic Press, San Diego, CA (1993).
14. Dichter, M. A. Rat cortical neurons in cell culture: culture methods, cell morphology, electrophysiology, and synapse formation. *Brain Res.* **149**: 279–293 (1978).
15. Hamill, O. P., A. Marty, E. Neher, B. Sakmann, and F. J. Sigworth. Improved patch-clamp techniques for high resolution current recording from cells and cell-free membrane patches. *Pfluegers Arch.* **319**:85–100 (1981).
16. Johnson, J. W., and P. Ascher. Equilibrium and kinetic study of glycine action on the *N*-methyl-D-aspartate receptor in cultured mouse brain neurons. *J. Physiol. (Lond.)* **455**:339–365 (1992).
17. Colquhoun, D., and F. J. Sigworth. Fitting and statistical analysis of single channel records, in *Single Channel Recordings* (B. Sakmann and E. Neher, eds.). Plenum Press, New York, 191–263 (1983).
18. Sigworth, F. J., and S. M. Sine. Data transformations for improved display and fitting of single-channel dwell time histograms. *Biophys. J.* **52**:1047–1054 (1987).
19. Vanecek, J., V. Krebs, E. Scheer, and T. Bieleke. A note on an apparatus for intracerebral injections in conscious mice. *J. Am. Pharm. Assoc.* **49**:178 (1960).
20. Tallarida, R. J., and R. B. Murray. *Manual of Pharmacologic Calculations with Computer Programs*, Ed. 2. Springer-Verlag, New York (1987).
21. Hille, B. *Ionic Channels of Excitable Membranes*, Ed. 2. Sinauer, Sunderland, MA, 390–422 (1992).
22. Adams, P. R. Voltage jump analysis of procaine action at frog end-plate. *J. Physiol. (Lond.)* **268**:291–318 (1977).
23. Ruff, R. L. The kinetics of local anesthetic blockade of end-plate channels. *Biophys. J.* **37**:625–631 (1982).
24. Warnick, J. E., M. A. Maleque, N. Bakry, A. T. Eldefrawi, and E. X. Albuquerque. Structure-activity relationships of amantadine. I. Interaction of the *N*-alkyl analogues with the ionic channels of the nicotinic acetylcholine receptor and electrically excitable membrane. *Mol. Pharmacol.* **22**:82–93 (1982).
25. Neher, E., and J. H. Steinbach. Local anaesthetics transiently block currents through single acetylcholine-receptor channels. *J. Physiol. (Lond.)* **277**:153–176 (1978).
26. Nowak, L., P. Bregestovski, P. Ascher, A. Herbet, and A. Prochiantz. Magnesium gates glutamate activated channels in mouse central neurones. *Nature (Lond.)* **307**:462–465 (1984).
27. Ascher, P., and L. Nowak. The role of divalent cations in the *N*-methyl-D-aspartate responses of mouse central neurones in culture. *J. Physiol. (Lond.)* **399**:247–266 (1988).
28. Jahr, C. E., and C. F. Stevens. A quantitative description of NMDA receptor-channel kinetic behavior. *J. Neurosci.* **10**:1830–1837 (1990).
29. Gibb, A. J., and D. Colquhoun. Activation of *N*-methyl-D-aspartate receptors by L-glutamate in cells dissociated from adult rat hippocampus. *J. Physiol. (Lond.)* **456**:143–179 (1992).
30. Koshelev, S., and B. Khodorov. Tetraethylammonium and tetrabutylammonium as tools to study NMDA channels of neuronal membrane. *Biol. Membr.* **9**:1064–1068 (1992).
31. Vorobjev, V. S., and I. N. Sharonova. Tetrahydroaminoacridine blocks and prolongs NMDA receptor-mediated responses in a voltage-dependent manner. *Eur. J. Pharmacol.* **253**:1–8 (1994).
32. Costa, A. C. S., and E. X. Albuquerque. Dynamic of the action of tetrahydro-9-aminoacridine and 9-aminoacridine on glutamatergic currents: concentration-jump studies in cultured rat hippocampal neurons. *J. Pharmacol. Exp. Ther.* **268**:503–514 (1994).
33. Benveniste, M., and M. Mayer. Trapping of glutamate and glycine during open channel block of rat hippocampal neuron NMDA receptors by 9-aminoacridine. *J. Physiol. (Lond.)*, in press.
34. Christine, C. W., and D. W. Choi. Effect of zinc on NMDA receptor-mediated channel currents in cortical neurons. *J. Neurosci.* **10**:108–116 (1990).
35. Donevan, S. D., S. M. Jones, and M. A. Rogawski. Arcaine blocks *N*-methyl-D-aspartate receptor responses by an open channel mechanism: whole-cell and single-channel recording studies in cultured hippocampal neurons. *Mol. Pharmacol.* **41**:727–735 (1992).
36. Wright, J. M., P. A. Kline, and L. M. Nowak. Multiple effects of tetraethylammonium on *N*-methyl-D-aspartate receptor-channels in mouse brain neurons in cell culture. *J. Physiol. (Lond.)* **439**:579–604 (1991).
37. Woodhull, A. M. Ionic blockade of sodium channel in nerve. *J. Gen. Physiol.* **61**:687–708 (1973).
38. Johnson, J. W., and P. Ascher. Voltage-dependent block by intracellular Mg^{2+} of *N*-methyl-D-aspartate-activated channels. *Biophys. J.* **57**:1085–1090 (1990).
39. Sabramaniam, S., S. D. Donevan, and M. A. Rogawski. Hydrophobic interactions of *n*-alkyl diamines with the *N*-methyl-D-aspartate receptor: voltage-dependent and -independent blocking sites. *Mol. Pharmacol.* **45**: 117–124 (1994).
40. Jahr, C. E. High probability opening of NMDA receptor channels by L-glutamate. *Science (Washington D. C.)* **255**:470–472 (1992).

Send reprint requests to: Jon W. Johnson, Department of Neuroscience, 446 Crawford Hall, University of Pittsburgh, Pittsburgh, PA 15260.